

RSC Advances



This is an *Accepted Manuscript*, which has been through the Royal Society of Chemistry peer review process and has been accepted for publication.

Accepted Manuscripts are published online shortly after acceptance, before technical editing, formatting and proof reading. Using this free service, authors can make their results available to the community, in citable form, before we publish the edited article. This *Accepted Manuscript* will be replaced by the edited, formatted and paginated article as soon as this is available.

You can find more information about *Accepted Manuscripts* in the [Information for Authors](#).

Please note that technical editing may introduce minor changes to the text and/or graphics, which may alter content. The journal's standard [Terms & Conditions](#) and the [Ethical guidelines](#) still apply. In no event shall the Royal Society of Chemistry be held responsible for any errors or omissions in this *Accepted Manuscript* or any consequences arising from the use of any information it contains.

Investigation of Substitution Effect on Poly(bis-3,4-ethylenedioxythiophene methine)s through Solid State Polymerization[†]

Kai Peng, Tong Pei, Zhaoxiang Li, Lili Huang, Jiangbin Xia*

5

Receipt/Acceptance Data [DO NOT ALTER/DELETE THIS TEXT]

Publication data [DO NOT ALTER/DELETE THIS TEXT]

DOI: 10.1039/c1cc000000x [DO NOT ALTER/DELETE THIS TEXT]

10 Thieno[3,4-b]-1,4-dioxin, 5,5'-methylenebis[2,3-dihydro] was chosen as a universal solid state polymerization (SSP) platform due to its readily synthesis procedure, further tunable substitution groups on CH₂ bridge and its excellent conjugated quinonoid structure of corresponding poly(bis-3,4-ethylenedioxythiophene methine). These monomers were designed by taking the steric effect and molecular flexibility into consideration and by carefully investigated under SSP. In addition, the aromatic moieties were firstly introduced in branch chain in this polymer matrix, which may offer amazing properties and further modification opportunities based on this unique platform. 15 Our results reveal that the substitution groups on the CH₂ bridge play an important role in SSP. The bulkier the substitution group and the longer effective halogen distance the monomers have, the higher onset temperature (T_{onset}) the SSP will have. Furthermore, the primitive dependence of T_{onset} with effective halogen distance was established.

Keywords: Solid state polymerization, Molecular flexibility, Poly(bis-3,4-ethylenedioxythiophene methine), Quinonoid structure

20

Introduction

Conductive & conjugated polythiophene have been intensely investigated due to its numerous application such as light-emitting device, supercapacitors, electrochromic devices, including organic photovoltaic cells.¹⁻⁵ Through rational design, it can be easily tailored and synthesized with outstanding and multi-functional properties. It is known that eliminating the hydrogen atoms from a thiophene ring can construct corresponding conducting polymer, take this into consideration, the synthesis methods mainly cover chemical oxidation polymerization, electropolymerization and photo-polymerization. Meanwhile, the metal-catalyzed polycondensation plays a key role in those neutral polymers synthesis. Recently, a new method of solid state polymerization (SSP)⁶⁻⁷ attracted much attention due to its solvent free, oxidant free and/or external applied potential free special features, which are required by traditional methods as mentioned above.

Recently, different from the popular longitudinal direction design concept, we and others proposed a new design strategy which is along with 3,4-Ethylenedioxythiophene (EDOT) parallel direction through introducing a flexible linker between EDOT units and it made great SSP success.⁸ Meanwhile, it is noticed

that the substitution group has great influence on SSP excluding the linker atoms effect. For instance, introduction of rigid benzene ring would increase the onset temperature of SSP (T_{onset}).^{8b} In addition, Perepichka group observed similar substitution steric effect that the fixed 5-member ring monomer was more stable than the molecule which is with free two methyl group attached on ethylene 2,3-dihydro-thieno[3,4-b][1,4]dioxine.^{7c} These interesting observation reminded us that it would be possible to accurate control SSP process by simply fixing the flexible linker, changing the monomers flexibility as well as their basic platform structures.

55 Except for obtaining crystals structures information based on non-conjugated platform of EDOT-CH₂-N(R)-CH₂-EDOT,^{8c} we stop further work on this system and switch our efforts to those one atom linker containing systems due to the generation of quinoidal structure of polymers. In addition, empirical rule for SSP for polythiophene synthesis can not be established due to lack of enough crystal data.

Here, thieno[3,4-b]-1,4-dioxin, 5,5'-methylenebis[2,3-dihydro] was chosen as a universal SSP platform due to its readily synthesis procedure, tunable substitution groups on CH₂ bridge and excellent photo physical & chemical properties in the corresponding poly(bis-3,4-ethylenedioxythiophene methine) matrix. All these monomers were designed mainly based on their steric effect, molecular flexibility and aromatic groups were introduced due to their abundance and versatility. Meanhile, due to the existence of conjugated quinonoid structure, poly(3,4-ethylenedioxythiophene methine) is a typical small band

*College of Chemistry and Molecular Science, Wuhan University, Wuhan 430072, China. E-mail: jbxia@whu.edu.cn (J. Xia)

Phone & Fax: 86-27-68756707

†Electronic supplementary information (ESI) available: CCDC 1410882-1410884, ¹H-NMR and ¹³C-NMR. For ESI and crystallographic data in CIF or other electronic format see DOI: 10.1039/c5ra...

gap polymer and appeared in 1980s,⁹ and it is poorly investigated for organic-electronic applications.¹⁰

This study would help us to establish the SSP database systematically and efficiently. Meanwhile, an equation has been primitively established to probe the relationship between effective halogen distances^{8b} with their T_{onset} , which would be a powerful tool to design or explain much more interesting samples for SSP.

Experimental

Materials. Chemicals were purchased from Wuhan Shenshi Chemicals Co., Ltd. and were used without further purification unless otherwise noted. EDOT was purchased from J & K. 5-Iodo-2,3-dihydro-thieno[3,4-b][1,4]dioxine (I-EDOT)¹¹ was synthesized according to previous report.

Monomer synthesis and solid state polymerization

Linking the thiophene moieties: synthesis of I₂-CH(R)-EDOT

General method

Monomers of I₂-CH(R)-EDOT were synthesized in accordance with previous method¹² as shown in Scheme 1. To a stirred solution of zinc chloride in hydrochloric acid between -8°C and -10°C, 5-iodo-3,4-ethylenedioxythiophene (2.0 eq.) was added over several minutes. Different aldehydes (1.0 eq.) were added dropwise over 60 min while maintaining the temperature around -10°C. The reaction mixture was stirred for 60 min while maintaining this temperature and then quenched with water and extracted with ether. The organic extract was washed with 5% sodium bicarbonate solution, and dried over magnesium sulfate, and then the solvent was evaporated. Purification by column chromatography (silica gel, light petroleum-CH₂Cl₂, 2 : 1) afforded white solid.

Monomer I₂-Ph-EDOT

White powder (24%), ¹H NMR: δ (300 MHz, DMSO-d₆) 7.24-7.31 (m, 3 H); 7.17-7.19 (m, 2 H); 5.76 (s, 1 H); 4.20 (m, 4 H); 4.16 (m, 4 H). ¹³C NMR: δ (300 MHz, DMSO-d₆) 144.4, 141.4, 137.8, 128.9, 127.9, 127.6, 123.0, 65.3, 64.7, 49.9.

Monomer I₂-Naph-EDOT

White powder (25%), ¹H NMR: δ (300 MHz, DMSO-d₆) 7.80-7.98 (m, 3 H); 7.42-7.58 (m, 3 H); 7.21 (m, 1 H); 6.47 (s, 1 H); 4.23 (m, 4 H); 4.18 (m, 4 H). ¹³C NMR: δ (300 MHz, DMSO-d₆) 144.4, 137.7, 137.2, 133.8, 130.7, 129.4, 128.3, 125.8, 124.8, 122.9, 65.3, 64.9, 50.1, 36.5.

Monomer I₂-Triph-EDOT

Yellowish powder (20%), ¹H NMR: δ (300 MHz, DMSO-d₆) 6.92-7.07 (m, 6 H); 6.70-6.85 (m, 6 H); 5.62 (s, 1 H); 4.15 (m, 4 H); 4.11 (m, 4 H); 2.18 (s, 6 H). ¹³C NMR: δ (300 MHz, DMSO-d₆) 147.8, 145.9, 145.2, 138.6, 133.6, 131.3, 129.7, 125.6, 124.2, 122.7, 66.1, 65.6, 50.8, 21.7.

Monomer I₂-Pr-EDOT

White powder (13%), ¹H NMR: δ (300 MHz, DMSO-d₆) 4.33-4.44 (t, 1 H); 4.21 (m, 4 H); 4.19 (m, 4 H); 1.70-1.84 (m, 2 H); 1.18-1.29 (m, 2 H); 0.80-0.90 (t, 3 H). ¹³C NMR: δ (300 MHz, DMSO-d₆) 144.2, 138.2, 137.6, 124.1, 65.3, 64.8, 48.3, 38.2, 34.9, 20.6, 13.8.

General Solid state polymerization

The SSP procedure was conducted according to previous method.^{7,8} In a closed 5 mL vial, the iodinated compounds

(100-300 mg) were incubated at 60-150°C for 2-24 h. The grounded polymers were additionally dried in vacuum at 80°C overnight, then stirred with hydrazine hydrate (50% aqueous solution, in CH₃OH) overnight, filtered, and washed with CH₃OH. At last, the vacuum drying afforded the nearly fully dedoped respective polymers.

Crystal Structure Determination

Intensity data for the obtained three crystals were collected by using Mo K α radiation ($\lambda = 0.7107 \text{ \AA}$) on a Bruker SMART APEX diffractometer equipped with a CCD area detector at rt. The crystallographic data and details of data collection for three monomers are given in Table S1 (see in the Supporting Information). Data sets reduction and integration were performed by using the software package SAINT PLUS.¹³ The crystal structure is solved by direct methods and refined by using the SHELXTL 97 software package.¹⁴

Other Characterizations

IR spectra for the characterization of the resulted polymers were recorded on a Perkin-Elmer FTIR spectrometer. Absorption spectra were measured on a Unicam UV 300 spectrophotometer at wavelengths from 300 to 1000 nm. Monomers were deposited by spin-coating or drop-casted with 0.5-3 wt% of CHCl₃ monomers solution on fluorine doped tin oxide (FTO) substrate or slide glasses. These monomer coated substrate were employed for SSP and then resulted polymers or polymer/FTO substrates. These products were used for XRD, UV-Vis or as working electrode for electrochemical measurements. For the three-electrode electrochemical measurements in 0.1 M LiClO₄ in acetonitrile, a 1 cm² area of FTO/Polymer substrate, platinum foil, and Ag/AgCl were served as the working, counter, and reference electrodes, respectively (CH Instruments 604D electrochemical system). X-ray diffraction (XRD) patterns were obtained by Bruker D8 advanced X-ray diffractometer by using Cu-K α radiation at rt. Thermogravimetric analysis (TGA) data were obtained from a SETSYS 16 with a heating rate of 10 °C/min in a nitrogen atmosphere. The molecular weight and molecular weight distribution of the polymers were determined by gel permeation chromatography (GPC) which was equipped with a Waters 2690 separation module and a Waters 2410 refractive index detector (Waters Co., Milford, MA). N,N-Dimethylformamide (DMF) was used as eluent at a flow rate of 0.5 ml min⁻¹ with the temperature maintained at 30 °C and the results were calibrated against polystyrene standards.

Results and Discussion

Synthesis of monomers and their solid state polymerization

All designed monomers were synthesized as shown in Scheme 1. Monomers of I₂-CH(R)-EDOT were obtained through the corresponding aldehydes reaction with I-EDOT in the existence of zinc chloride in hydrochloric acid. It is noted that the aromatic aldehydes show better yields compared with alkyl aldehyde. SSP results show that all monomers can successfully form corresponding polymers under heat treatment with different T_{onset} and also indicate that the substitution groups play a key role in their SSP behavior. It is interesting that after introducing of propyl group, I₂-Pr-EDOT requires the lowest T_{onset} of 70 °C while others need higher temperature in range of 80-130 °C. It appears that the bulkier aromatic group the monomer has, the

higher T_{onset} it needs. Detailed analysis & discussion concerning
190 of effective halogen distance and the relationship with T_{onset} will
be done in the crystal structure section. These interesting results
encourage us to the further explore much more acutely
controllable and fine tunable thiophene monomers for SSP.

195 XRD Patterns of monomers and respective polymers

As shown in Fig. 1, except for I₂-Pr-EDOT, most monomers
show typical sharp peaks in the rage of 5-50°, which are quite
consistent with their simulated results through their crystal structure
data. Because of the wax-state at room temperature,
200 I₂-Pr-EDOT's XRD shows wide peak around 23°. After SSP,
polymers show broad peak around 24.0°, 22 and 26° for
P(Nap-EDOT), P(TriPh-EDOT) and P(Pr-EDOT) respectively,
while in the case of P(Ph-EDOT), it shows poor resolution peak
in its XRD pattern. All these results indicate that substituted
205 groups on CH₂-bridge have big effect on chain packing^{9e} in
poly(bis-3,4-ethylenedioxythiophene methine) matrixes.

In order to further investigate what happened during SSP
procedure, *in-situ* XRD measurement was carried out for those
typical monomers of I₂-Ph-EDOT and I₂-Nap-EDOT, which their
210 crystals were obtained for further analysis. In addition, their most
crystal phases were labeled according to their crystal simulated
results. As shown in Fig. 2, it is obvious that the drastic intensity
decrease for (321) phase was observed at the initial one hour's
polymerization for monomer of I₂-Ph-EDOT while (421) phase's
215 intensity decrease was found along with the disappearance of
(401) phase within two hours of SSP. In addition, (420) phase
was decreased or even disappeared within three hours.
Meanwhile, in the case of I₂-Nap-EDOT, the drastic intensity
decrease of (1,0,-2), (0, 2, 2), (4,1,0) and (1,2,4) phases were
220 observed at the initial 2 hours' polymerization. In addition, (222)
phase was decreased within eight hours heat-treatment.

Solution UV-Vis spectra for those polymers

Compared with typical insoluble PEDOT polymer, these
225 monomers show small solubility in THF or DMF solvents.
Therefore, their solution absorption spectra and those of
hydrazine treated samples were presented in Fig. 3. It is clear that
all polymers show typical p-type featured character while their
neutral type polymers were obtained after hadrazene treatment
230 due to the observation of drastic intensity drop at near-IR region
around 700-1400 nm.^{15,16} Among those SSP generated polymer
solutions' absorption spectra, most of them show peak at 760 nm
except that P(Nap-EDOT) exhibits a peak at longer wave length
of 1000 nm. It indicates that P(Nap-EDOT) has the highest
235 polaron or charge carrier density.

As for those neutral polymers, it has big difference compared
with poly(3,4-ethylenedioxythiophene methine) which has typical
strong peak at longer wavelength of 1000 nm.^{12b} We attribute this
to the less quinonoid structure in these
240 poly(bis-3,4-ethylenedioxythiophene methine)s chain because of
their repeat unit of bis-EDOT other than EDOT. Briefly, the
introduction of benzene and naphthalene generates wide
absorption range with well resolved peaks at 470 and 493 nm
respectively. However, triphenylamine group results in a red
shifted curve with two peaks at 540 nm and a shoulder peak
245 around 650 nm. However, no distinct peak was observed for
P(Pr-EDOT) as shown in Fig. 3d. Their detailed parameters of

optical properties were summarized in Table 1. These absorption
spectra results indicate that the substitution groups on CH₂-bridge
250 have drastic effect on polymers optical properties, which may
offer much modification opportunity¹⁷ for different functional
usage.

FTIR Spectroscopy

255 A comparison of the FTIR spectra of these polymers is shown in
Fig. 4. Except for P(Ph-EDOT), most polymers have peaks
around 1471, 1434, and 1360 cm⁻¹ originated from the stretching
of C=C and C-C in the thiophene ring^{18,19}. Meanwhile, all
polymers demonstrate the featured peaks around 696 cm⁻¹ related
260 to in-plane deformation of C-S-C of thiophene ring.¹⁸ In the case
of P(TriPh-EDOT), it shows distinct strong sharp peak at 2920
and 2870 cm⁻¹, which are assigned to CH₃ stretching modes.²⁰ In
addition, due to the existence of C-N bond, C-N and C-N-C bend
modes at 1321 and 924 cm⁻¹ were observed.²¹

Cyclic voltammetry behavior of the polymers

The CV curves are shown in Fig. 5, with the corresponding data
summarized in Table 1. It is obvious that except for P(Pr-EDOT),
all polymer films show typical CV curves which were commonly
270 observed based on PEDOT. It indicates that such kind of
polymers may have great potential usage in capacitance charge
storage devices such as lithium battery, fuel cell and catalytic
electrode materials. Meanwhile, most polymers have similar
initial oxidation potential around 0 V vs Ag/AgCl while
275 P(Pr-EDOT) has higher initial oxidation potential of 0.32 V,
revealing that the introduction of propyl on CH₂ bridge will cause
more difficulty for oxidization. In addition, P(TriPh-EDOT)
shows initial oxidation potential around 0.18 V with an additional
oxidation potential of 0.8 V vs Ag/AgCl, which is assigned to N
280 oxidation^{22,23} in the polymer matrix. Furthermore, the N involved
peak shows typical reversible redox behavior, indicating that it is
a good candidate for charge storage or other redox alternatives in
some other electrochemical devices.

Furthermore, according to their CV curves, the primitive
285 charge storage capability sequence of the polymer is
P(Nap-EDOT) > P(Ph-EDOT) > P(TriPh-EDOT) > P(Pr-EDOT).
In addition, it is noticed that previous result indicates that the
poly(CH₂-EDOT)^{8a} with non-substitution on CH₂ bridge has good
electrochemical behavior, revealing that alkyl chain may destroy
290 quinonoid structure and lead to poor conjugation in the polymer
matrix to some extent. Therefore, the aromatic ring in polymer
matrix would enhance the quinonoid conjugation and the
stabilization of charge carrier in polymer matrix.

Crystallographic X-ray Analysis

295 Three single crystals of the monomers were obtained and studied
by X-ray analysis (shown in Figure 6-9) for further understanding
of the structural requirements for SSP. Though all monomers are
designed based on the same platform of EDOT-CH(R)-EDOT,
300 their crystal structures are quite different and their parameters are
listed in Table S1. In addition, the substitution of R has big effect
on I/I distances in monomers as shown in Fig 6. Their I/I
distances were derived from corresponding molecules structures
and it is found that the bulkier substitution group generates longer
305 intramolecular I/I distance.

The Fig. 6 shows the monomers structure and those intramolecular distance and angles information are derived from crystals and listed in Table 2. It is obvious that along with the introduction of the bulkier substitution groups, the I_1/I_2 and S_1/S_2 intramolecular distance increase gradually while the bridge length of (C-CH(R)-C) almost keep the original distance of 2.50 Å with an angle of 112.00° for \angle C-CH(R)-C. Meanwhile, angles of \angle $S_1C_7S_2$ and \angle $I_1C_7I_2$ increase greatly along with the introduction of bulkier substitution group. All these facts reveal that the steric effect plays an important role in their monomers structures. In addition, the long flexible chain may not have big effect on it if further increase alkyl chain length.

As shown in Fig. 7, no dimer exists in I_2 -Pr-EDOT crystal, but it is with the first and the second closest Hal/Hal distance of 4.267 and 4.878 Å respectively, accompanying with C11-C11 and C11-C1 contact of 7.681 and 5.517 Å respectively. Meanwhile, it has the third closest Hal/Hal distance of 6.305 Å, accompanying with the second shortest C-C (C1-C1) contact of 4.820 Å. It is found that the first polymerization pathway (formation of a spring circle, shown in Fig. 7c.) involves sole I/I distance of 4.878 Å while the second polymerization pathway (shown in Fig. 7d) involves two I/I distances of 4.267 Å and 6.305 Å, indicating that the formal pathway is the preferred one with the effective halogen distance of 4.878 Å for SSP.

As shown in Fig. 8, it is with the first and the second closest Hal/Hal distance of 4.374 and 4.514 Å respectively, accompanying with C19-C1 and C19-C1 contact of 5.460 and 5.298 Å respectively. Meanwhile, it has the third closest Hal/Hal distance of 6.115 Å with the corresponding shortest C-C (C19-C19) contact of 4.957 Å. Similar like I_2 -Pr-EDOT, it forms a spring circle with the first polymerization pathway along with c -axil direction as shown in Fig. 8c. In addition, the second possible polymerization pathways along with b -axil direction was demonstrated in Fig 8d. Interestingly, the sole I/I distances of 4.374 and 4.514 Å are involved for these two pathways respectively, so taking this into consideration, the first pathway is a preferred one.

As shown in Fig. 9, the first and the second closest Hal/Hal distance for I_2 -Nap-EDOT are 5.242 and 5.375 Å respectively, accompanying with C1-C1 and C13-C13 contact of 5.941 and 4.839 Å respectively. Meanwhile, it has the third closest Hal/Hal distance of 6.522 Å with corresponding the C13-C1 contact of 7.306 Å. Compared with the above two monomers, its first Hal/Hal distance is very long and it is the largest one among all obtained monomers by other groups including ours.⁹ After carefully analysis, a plausible polymerization pathway along with b -axis direction was presented in Fig. 9c. In this pathway, it involves two I/I distances of 5.242 Å and 5.375 Å with its effective halogen distance of 5.375 Å.

The dependence of effective I/I distances with their onset temperature of SSP

So far, T_{onset} , effective halogen distance^{8b} have been defined T_{onset} , effective halogen distance^{8b} for SSP and SSP model^{8b} have been proposed a for rigid and flexible monomers. Here we try to establish an equation to probe its relationship between effective halogen/halogen distances and their T_{onset} according to these obtained crystals data. The dependence of effective I/I distance with their T_{onset} were shown in Fig. 10 (data derived from those

samples was presented in Table S2). According to the fitted line, it gives an equation of $y = 26.1x - 31.5$, with R of 0.92, revealing that increasing 1 Å of effective I/I distance needs the elevated T_{onset} of around 26°C.

Meanwhile, it is noticed that I_2 -Pr-EDOT's effective halogen distance is longer than that of I_2 -Ph-EDOT while the former shows higher T_{onset} than that of the latter. Due to the existence of alkyl chain, it would weaken inter-molecule π - π stacking in the crystal and result in lower T_{onset} . A prediction would be made that I_2 -Triph-EDOT's effective I/I distance is over 5.5 Å because of its highest T_{onset} of 120 °C among all monomers. Taking SSP condition range from room temperature to 300 °C into consideration, heat process would drastically control molecule movement and SSP should have bright future in getting great success for the synthesis of other polythiophene systems.

Molecule weight information and thermal stability TGA analysis

Though solution absorption spectra of P(Ph-EDOT), P(Nap-EDOT), P(Triph-EDOT) can be obtained, their molecule weight information cannot be measured due to their limited solubility. M_n of 2.15 kg mol⁻¹ with PDI of 1.64 indicates that the P(Pr-EDOT) has a repeat units of 6, which is a litter bit shorter than that of P(3-alkyl-EDOT)^{8c} with CH₂-N(R)-CH₂ linker. The thermal stability of the polymers was investigated with thermogravimetric analysis (TGA). The 5% weight-loss temperatures for P(Pr-EDOT), P(Ph-EDOT), P(Nap-EDOT), P(Triph-EDOT) were 238, 244, 229 and 273°C, respectively, indicating that the introduction of triphenylamine moiety would enhance thermal stability greatly.

Conclusions

In this work, several new thiophene derivatives were synthesized based on EDOT-CH(R)-EDOT platform and successfully employed in SSP. Due to their quinonoid structures, our results may allow us to drastically expand the SSP scope and to prepare new types of poly(bis-3,4-ethylenedioxythiophene methine)s. Our results show that these polymers have excellent optical and electrical properties, implying that their will be great application potential with promising future, though they were ignored at present. Moreover, the relationship between monomers' effective halogen distance and their T_{onset} was established, revealing of SSP's powerful molecule arrangement & interaction.

Acknowledgments

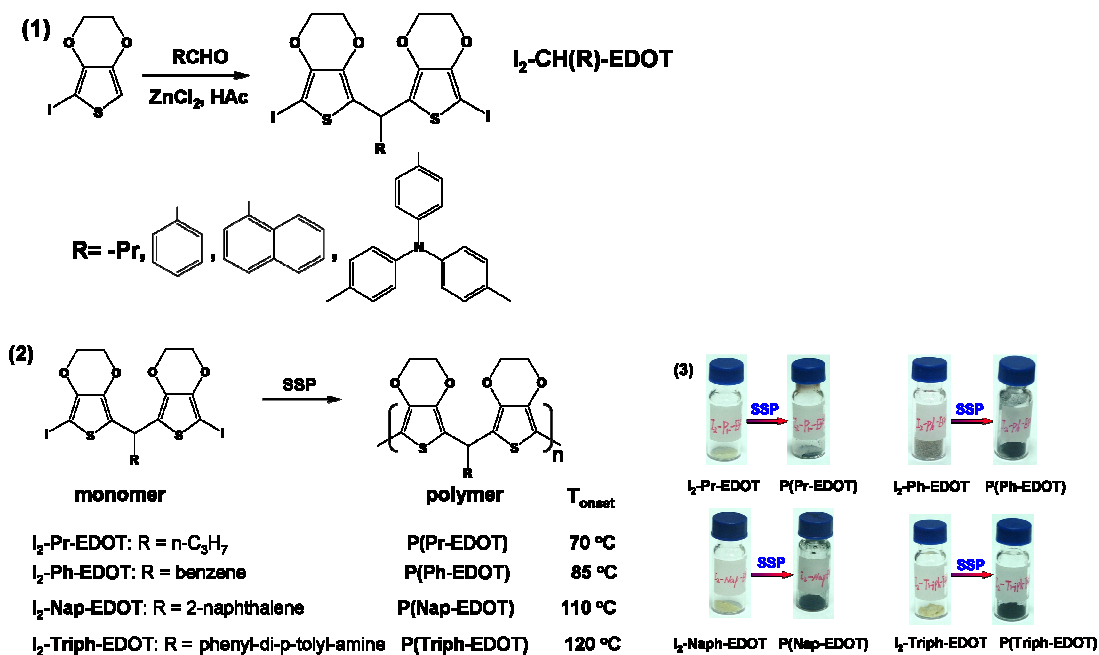
This work was supported by the Natural Science Foundation of China (21371138) the Funds for Creative Research Groups of Hubei Province (2014CFA007), the Fundamental Research Funds for the Central Universities (2042015kf0180) of China and Large-scale Instrument And Equipment Sharing Foundation of Wuhan University.

References

1. Q. Pei, Y. Yang, G. Yu, C. Zhang and A. J. Heeger, *J. Am. Chem. Soc.*, 1996, **118**, 3922.
2. H. L. Wang, F. Huang, A. G. MacDiarmid, Y. Z. Wang, D. D. Gebler and A. J. Epstein, *Synth. Met.*, 1996, **80**, 97.

3. A. Laforgue, P. Simon, C. Sarrazin and J.-F. Fauvarque, *J. Power Sources*, 1999, **80**, 142.
4. W. Lu, F. Andrei, B. Qi, S. Elisabeth, M. Benjamin R. J. Ding, S. Geoffrey, M. Jakub, D. Zhou, W. Gordon., M. Douglas, F. Stewart and F. Maria, *Science*, 2002, **297**, 983.
5. (a) L. S. Roman, M. R. Andersson, T. Yohannes and O. Inganaes, *Adv. Mater.*, 1997, **9**, 1164; (b) J. Xia, N. Masaki, K. Jiang and S. Yanagida, *J. Mater. Chem.*, 2007, **17**, 2845; (c) J. Xia, N. Masaki, M. Lira-Cantu, Y. Kim, K. Jiang and S. Yanagida, *J. Am. Chem. Soc.* 2008, **130**, 1258; (d) J. Xia, L. Chen and S. Yanagida, *J. Mater. Chem.*, 2011, **21**, 4644. (e) L. Chen, J. Jin, X. Shu and J. Xia, *J. Power. Sources*, 2014, **248**, 1234.
6. (a) H. Meng, D. F. Perepichka and F. Wudl, *Angew. Chem. Int. Ed.*, 2003, **42**, 658; (b) H. Meng, D. F. Perepichka, M. Bendikov, F. Wudl, G. Z. Pan, W. Yu, W. Dong and S. Brown, *J. Am. Chem. Soc.*, 2003, **125**, 15151.
7. (a) H. J. Spencer, R. Berridge, D. J. Crouch, S. P. Wright, M. Giles, I. McCulloch, S. J. Coles, M. B. Hursthouse and P. J. Skabara, *J. Mater. Chem.*, 2003, **13**, 2075; (b) A. Patra, Y. H. Wijsboom, S. S. Zade, M. Li, Y. Sheynin, G. Leitus and M. Bendikov, *J. Am. Chem. Soc.*, 2008, **130**, 6734; (c) M. Lepeltier, J. Hiltz, T. Lockwood, F. Bélangier-Gariépy and D. F. Perepichka, *J. Mater. Chem.*, 2009, **19**, 5167; (d) A. Patra, Y. H. Wijsboom, G. Leitus and M. Bendikov, *Chem. Mater.*, 2011, **23**, 896; (e) S. Chen, J. Xu, B. Lu, X. Duan and F. Kong, *Adv. Mater. Res.*, 2011, **239–242**, 924; (f) S. Chen, B. Lu, X. Duan and J. Xu, *J. Polym. Sci. Part A, Polym. Chem.*, 2012, **50**, 1967.
8. (a) C. Tusy, L. Huang, J. Jin and J. Xia, *RSC Adv.*, 2014, **4**, 8011; (b) C. Tusy, L. Huang, K. Peng and J. Xia, *RSC Adv.*, 2014, **4**, 29032; (c) C. Tusy, L. Huang, K. Peng and J. Xia, *RSC Adv.*, 2015, **5**, 16292; (d) A.-L. Barrès, M. Allain, P. Frère and P. Batail, *Isr. J. Chem.* 2014, **54**, 689.
9. (a) S. A. Jenekhe, *Nature*, 1986, **322**, 345; (b) W. -C. Chen, C. -L. Liu, C.-T. Yen, F.-C. Tsai, C. J. Tonzola, N. Olson and S. A. Jenekhe, *Macromolecules* 2004, **37**, 5959; (c) M. B. Zaman and D. F. Perepichka, *Chem. Commun.*, 2005, 4187; (d) A. Abdolmaleki, Z. Mohamadi, B. Rezaei and N. Askarpour, *Polym. Bull.*, 2013, **70**, 665; (e) S. Ahn, K. Yabumoto, Y. Jeong and K. Akagi, *Polym. Chem.*, 2014, **5**, 6977.
10. (a) H. Neugebauer, C. Kvarnström, C. Brabec, N. S. Sariciftci, R. Kiebooms, F. Wudl and S. Luzzati, *J. Chem. Phys.*, 1999, **110**, 12108; (b) T. Umeyama, Y. Watanabe, M. Oodoi, D. Evgenia, T. Shishido and H. Imahori, *J. Mater. Chem.*, 2012, **22**, 24394.
11. V. Lemau de Talance, M. Hissler, L.-Z. Zhang, T. Karpati, L. Nyulaszi, D. Caras-Quintero, P. Baeuerle and R. Reau, *Chem. Commun.*, 2008, **19**, 2200.
12. (a) K. J. Hoffmann, L. Knudsen, E. J. Samuelsen and P. H. J. Carlsen, *Synth. Metal.*, 2000, **114**, 161; (b) T. Benincori, S. Rizzo, F. Sannicolo, G. Schiavon, S. Zecchin and G. Zotti, *Macromolecules*, 2003, **36**, 5114.
13. G. M. Sheldrick, SHELXTL, Version 6.14, Bruker Analytical X-ray Instruments, Inc, Madison, WI, USA, 2003.
14. G. M. Sheldrick, *Acta Crystallogr. Sect. A*, 2008, **A64**, 112.
15. Y. Xia, A. G. MacDiarmid and A. J. Epstein, *Macromolecules*, 1994, **27**, 7212.
16. D. Hohnholz, A. G. MacDiarmid, D. M. Sarno and Jr. W. E. Jones, *Chem. Commun.*, 2001, 2444.
17. B. Bhushan, S. K. Kumar, S. S. Talwar, T. Kundu and B. P. Singh, *Appl. Phys. B*, 2012, **109**, 201.
18. C. Kvarnström, H. Neugebauer, S. Blomquist, H. J. Ahonen, J. Kankare and A. Ivaska, *Electrochim. Acta*, 1999, **44**, 2739.
19. G. Louarn, J. Kruszka, S. Lefrant, M. Zagorska, I. Kulszewicz-Bayer and A. Pron, *Synth. Met.*, 1993, **61**, 233.
20. M. S. Agashe and C. I. Jose, *J. Chem. Soc. Faraday Trans. 2*, 1977, **73**, 1232.
21. I. Reva, L. Lapinski, N. Chattopadhyay and R. Fausto, *Phys. Chem. Chem. Phys.*, 2003, **5**, 3844.
22. T. L. Macdonald, W. G. Gutheim, R. B. Martin and F. P. Guengerich, *Biochem.*, 1989, **28**, 2071.
23. J. W. Arbogast, C. S. Foote and M. Kao, *J. Am. Chem. Soc.*, 1992, **114**, 2277.

CREATED USING THE RSC ARTICLE TEMPLATE (VER. 2.1) - SEE WWW.RSC.ORG/ELECTRONICFILES FOR DETAILS



Scheme 1. Synthesis of the monomers, corresponding polymers and digital images of crystals of monomers and respective polymers.

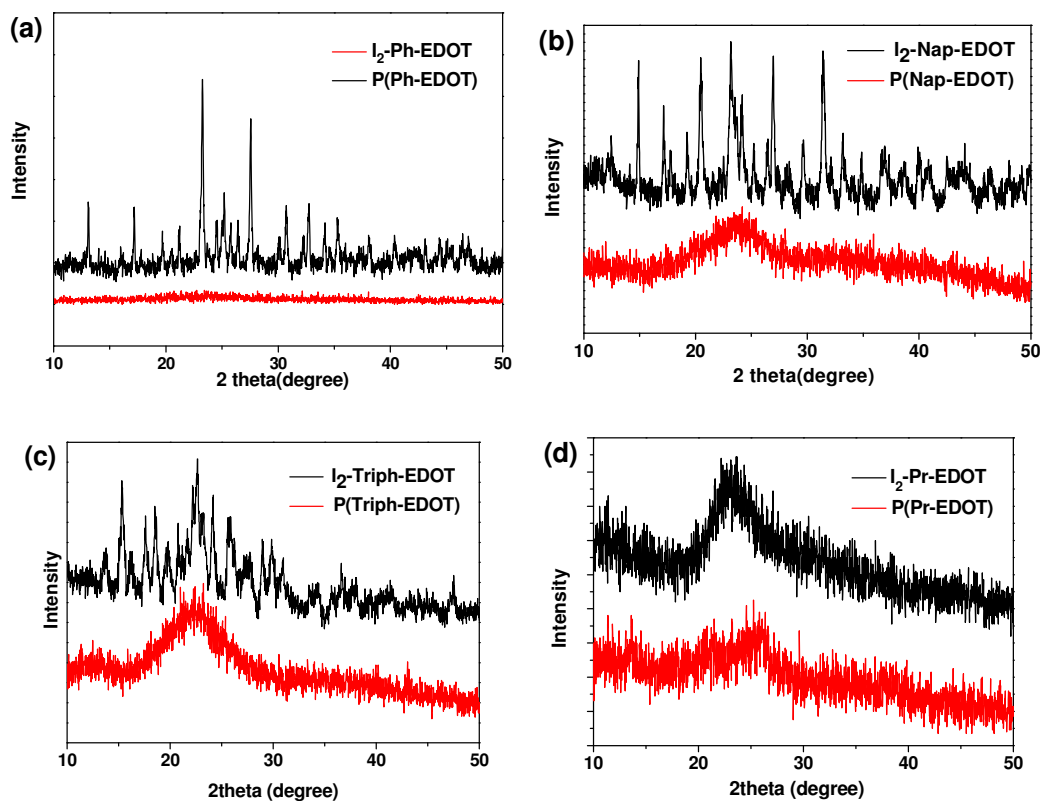


Fig. 1 XRD spectra of monomers and corresponding polymers.

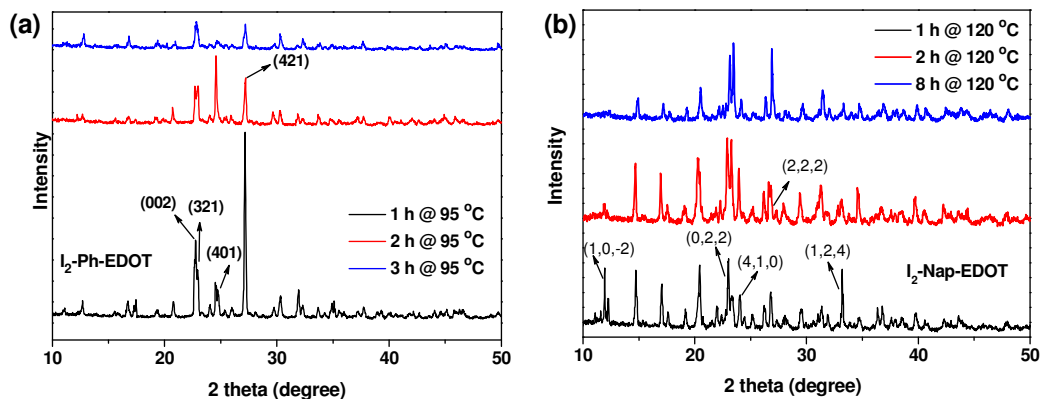


Fig. 2 In situ-XRD patterns for (a) I₂-Ph-EDOT and (b) I₂-Nap-EDOT.

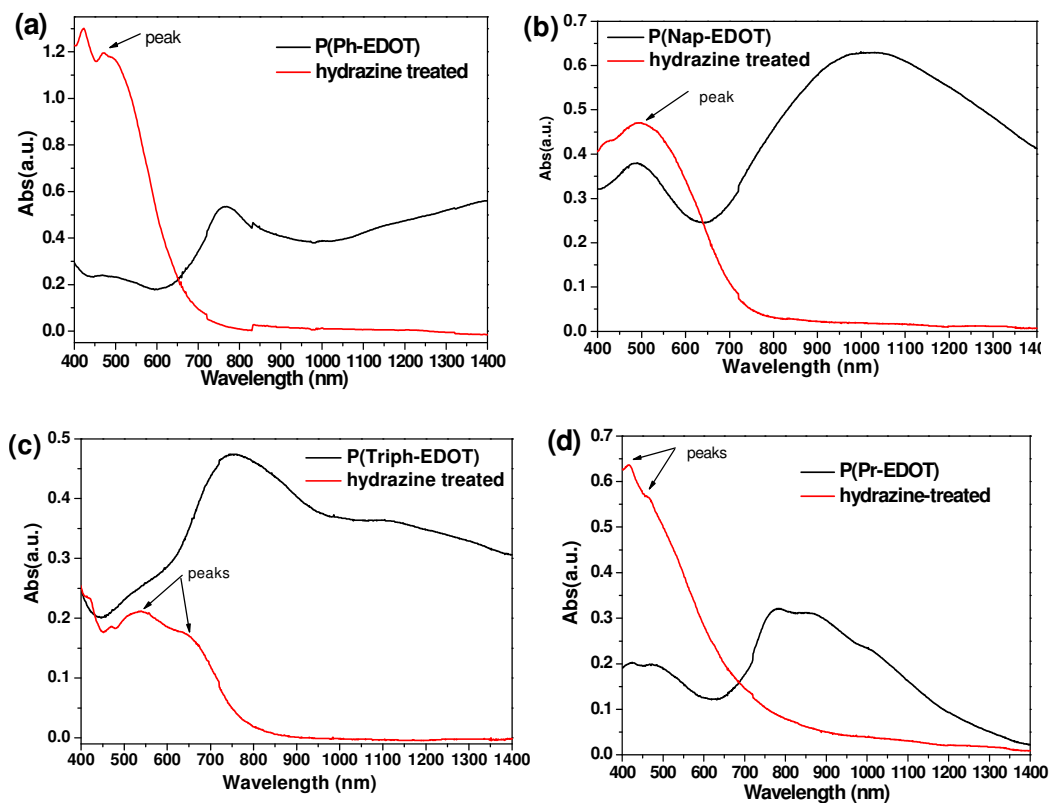


Fig. 3 Solutions absorption spectra of the polymer solutions obtained by SSP and dedoped polymers.

CREATED USING THE RSC ARTICLE TEMPLATE (VER. 2.1) - SEE WWW.RSC.ORG/ELECTRONICFILES FOR DETAILS

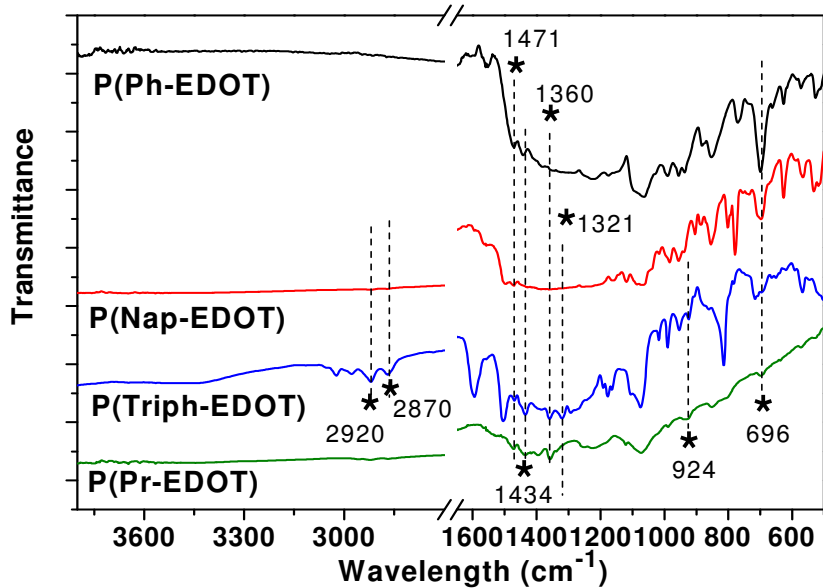


Fig. 4 FTIR spectra for these Poly(bis-3,4-ethylenedioxythiophene methine)s obtained through SSP.

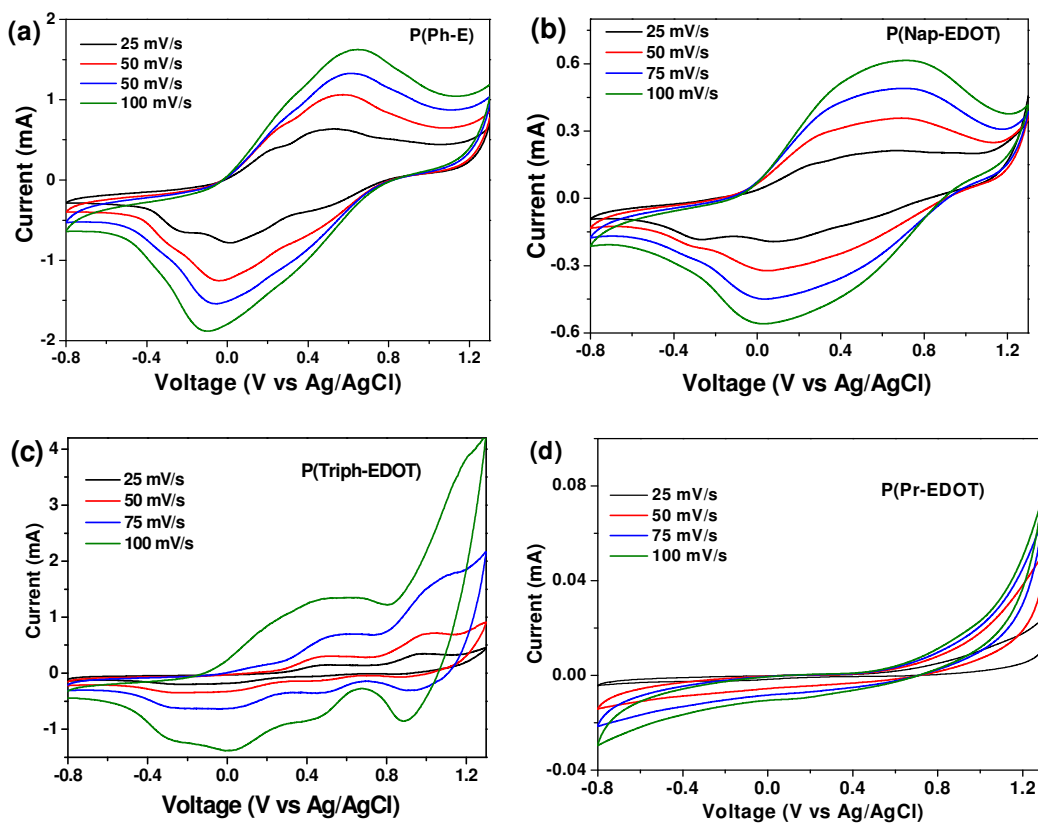


Fig. 5 The CVs of Polymers films in acetonitrile solution containing 0.1 M Bu_4NClO_4 taken at various scan rates.

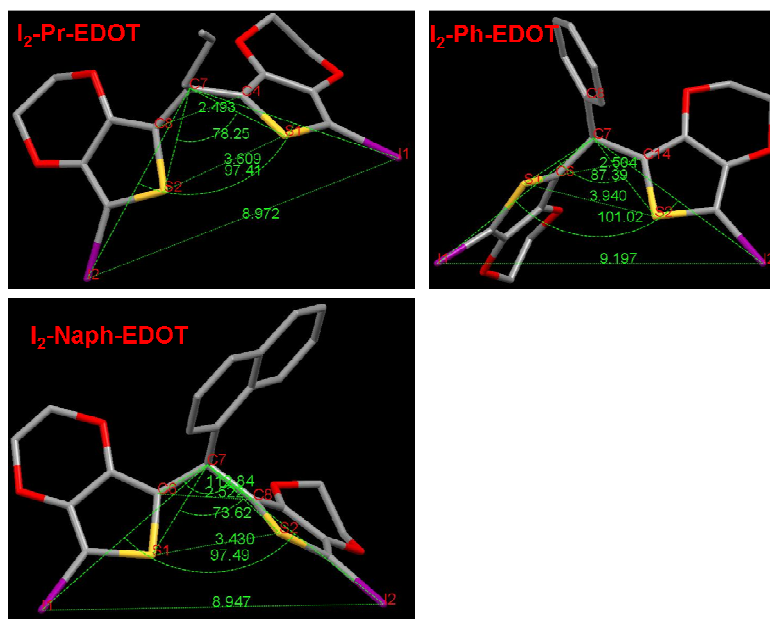


Fig. 6 Intermolecular I/I distance and different angles in these monomers.

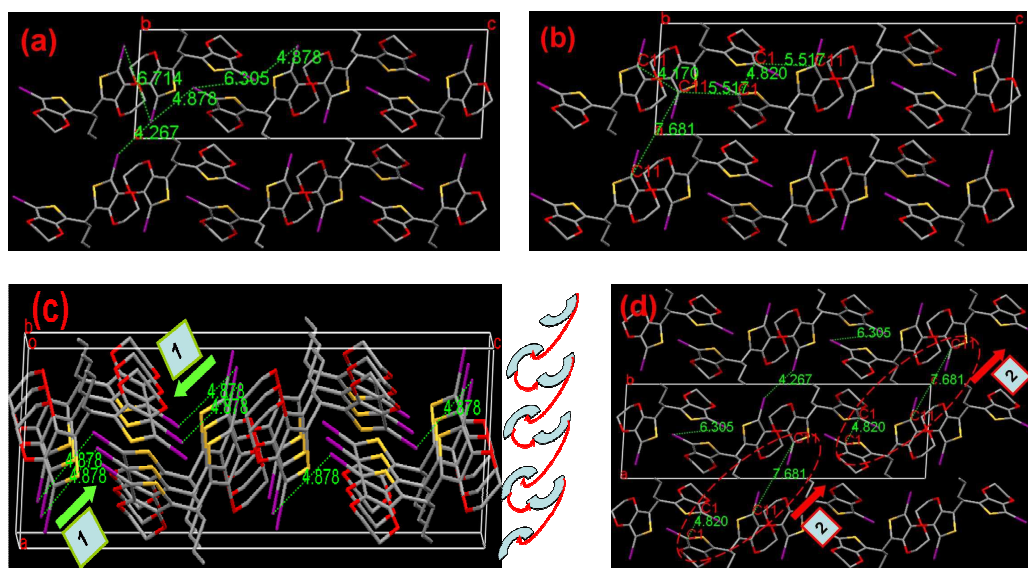


Fig. 7 Single-crystal X-ray structure of compound I₂-Pr-EDOT. (a) view of I/I distance, (b) view of corresponding C/C contact distance, (c) crystal packing viewed along the *b*-axis, proposed the first polymerization pathway and involved I/I and C/C contact distances, (d) proposed the second polymerization pathway. Hydrogen atoms are omitted for clarity; I, purple; S, yellow and C, gray.

CREATED USING THE RSC ARTICLE TEMPLATE (VER. 2.1) - SEE WWW.RSC.ORG/ELECTRONICFILES FOR DETAILS

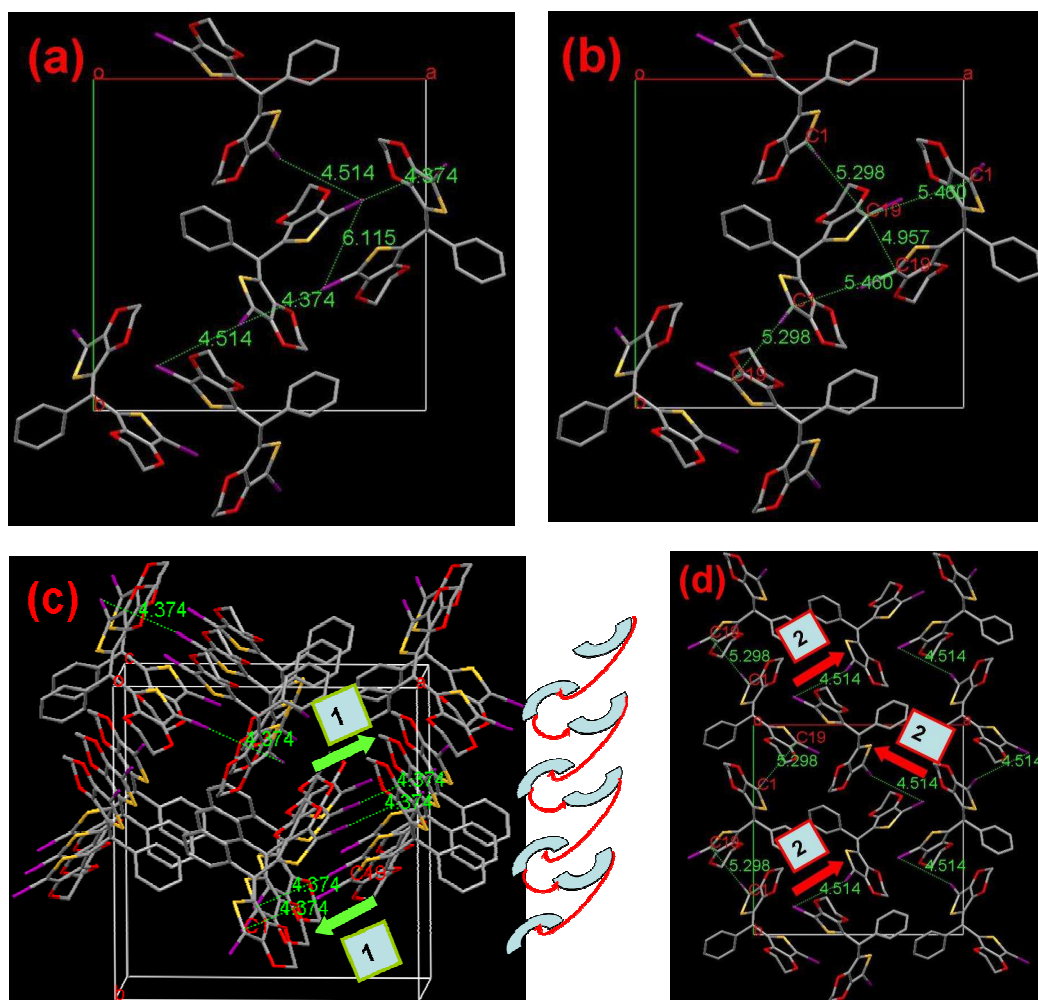


Fig. 8 Single-crystal X-ray structure of compound I₂-Ph-EDOT. (a) view of I/I distance, (b) view of corresponding C/C contact distance, (c-d) crystal packing viewed along the *c*-axis, proposed first polymerization pathway and involved I/I and C/C contact distance, (e) proposed the second polymerization pathway. Hydrogen atoms are omitted for clarity: I, purple; S, yellow and C, gray.

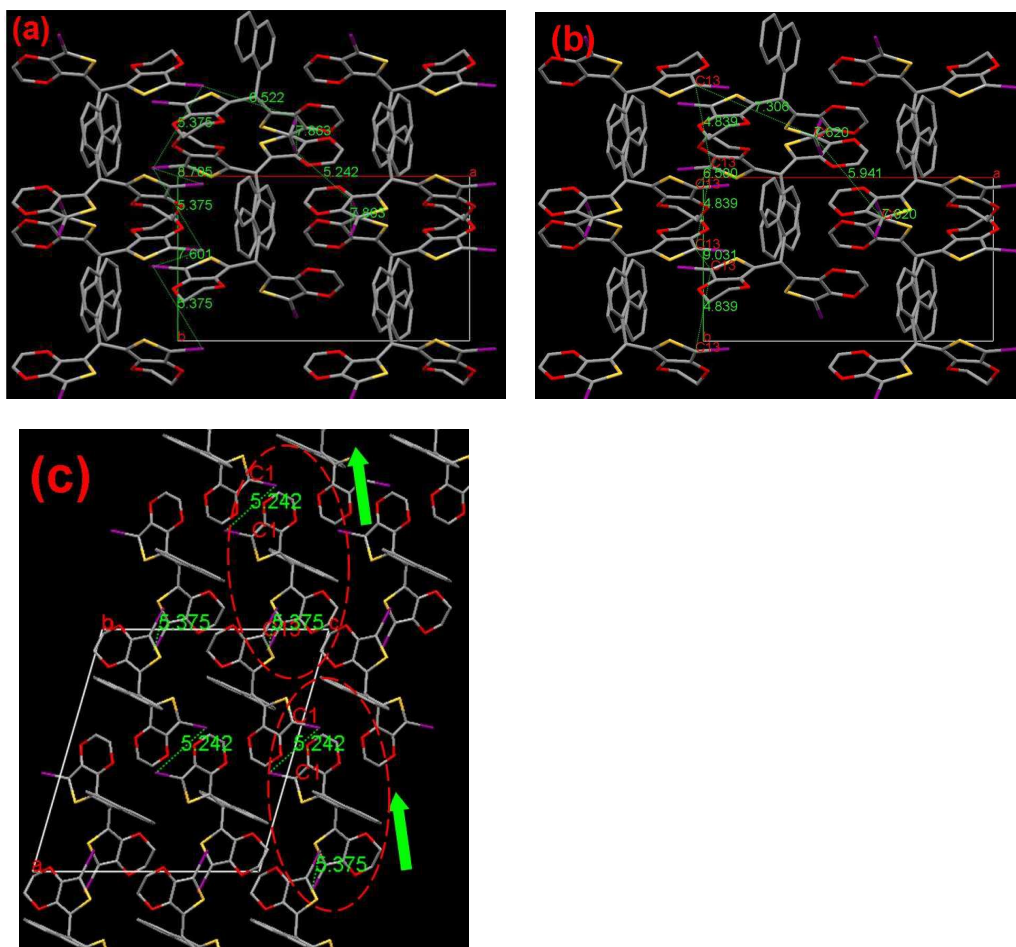


Fig. 9 Single-crystal X-ray structure of compound I₂-Nap-EDOT. (a) view of I/I distance, (b) view of corresponding C/C contact distance, (c) crystal packing viewed along the *b*-axis, proposed plausible polymerization pathway and involved I/I and C/C contact distances. Hydrogen atoms are omitted for clarity: I, purple; S, yellow and C, gray.

CREATED USING THE RSC ARTICLE TEMPLATE (VER. 2.1) - SEE WWW.RSC.ORG/ELECTRONICFILES FOR DETAILS

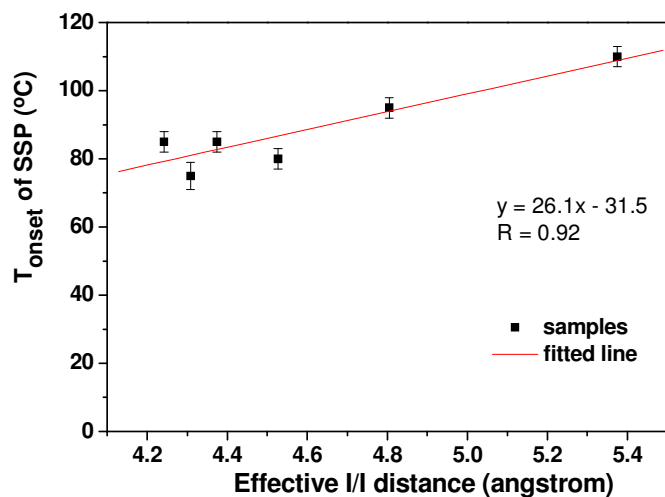


Fig. 10 Linear dependence of effective I/I distance with T_{onset} of SSP

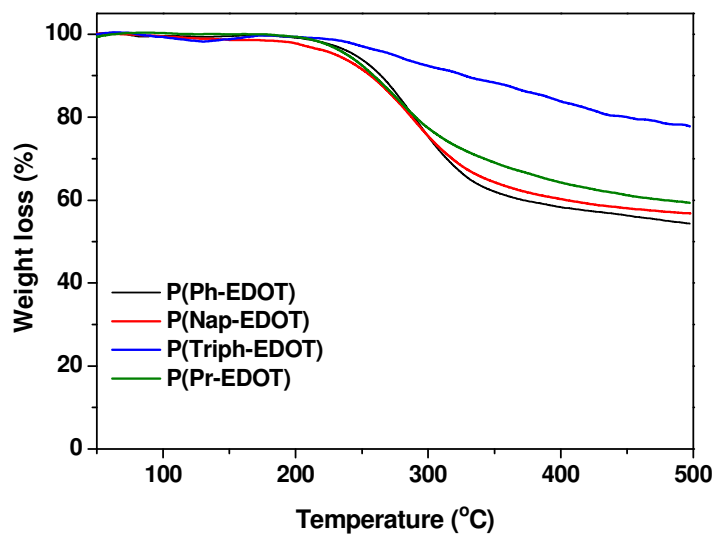


Fig. 11 TGA of the polymers under N₂ atmosphere with heating rate of 10°C/min

Table 1 Optical and electrochemical data for all neutral polymers

	Conversion for 24 h (temperature)	Abs. λ_{max} /nm film	Abs. λ_{edge} /nm film	E_{gap}^a (eV)	HOMO (eV)	LUMO ^b (eV)
P(Ph-EDOT)	> 90 %, 110 °C	422, 470	695	1.78	-4.38	-2.60
P(Nap-EDOT)	> 90 %, 130 °C	493	724	1.71	-4.33	-2.62
P(Triph-EDOT)	> 90 %, 150 °C	540	785	1.58	-4.54	-2.96
P(Pr-EDOT)	> 90 %, 100 °C	420, 465	690	1.80	-4.68	-2.88

^a Determined from the onset wavelength in the absorption spectra of film samples. ^b Determined from HOMO levels and optical bandgaps.

Table 2 Intramolecular halogen distance and angles

	Distance (Å)			Angles (°)		
	I ₁ /I ₂	S ₁ /S ₂	bridge length (C-C _{H(R)} -C)	\angle C-C _{H(R)} -C	\angle S ₁ C ₇ S ₂	\angle I ₁ C ₇ I ₂
I ₂ -Pr-EDOT	8.972	3.609	2.493 (C ₄ /C ₈)	111.92 (\angle C ₈ C ₇ C ₄)	78.25	97.41
I ₂ - Ph-EDOT	9.197	3.940	2.504 (C ₆ /C ₁₄)	112.00 (\angle C ₆ C ₇ C ₁₄)	87.39	101.02
I ₂ -Nap-EDOT	8.947	3.430	2.522 (C ₆ /C ₈)	112.84 (\angle C ₆ C ₇ C ₈)	73.62	97.49

Table 3 Selected I/I and C-C contact distance (Å) for the reported crystals

Molecules parameters	I ₂ - Ph-EDOT	I ₂ - Nap-EDOT	I ₂ -Pr-EDOT
shortest I/I distance	4.374 ^a	5.242	4.267
2 nd shortest I/I distance	4.514	5.375 ^a	4.878 ^a
3 rd shortest I/I distance	6.115	6.522	6.305
C-C contact shortest distance	4.957	4.839	4.170
C-C contact 2 nd shortest distance	5.298	5.941	4.820
longer than 2r _w of iodine ^b	10.9%	34.4%	21.9%
T _{onset} of SSP (°C)	85	110	70

^aEffective Hal/Hal distance

^b2r_w of iodine: double van der Waals radius of iodine: 4.0 Å

GRAPHICAL ABSTRACT

Investigation of Substitution Effect on Poly(bis-3,4-ethylenedioxythiophene methine)s through Solid State Polymerization

Kai Peng, Tong Pei, Zhaoxiang Li, Lili Huang, Jiangbin Xia*

EDOT-*CH(R)*-EDOT was chosen as a prototype model monomer for solid state polymerization (SSP). The aromatic moieties were first introduced in branch chain in the polymer matrix, which may offer amazing properties and further modification opportunities based on this unique platform.

